STRENGTHENING AND HAZARD MITIGATION OF URM WALLS USING FRP

A. A. Hamid [1] , W. W. El-Dakhakhni [2], Z. H.R. Hakam [3] and M. Elgaaly [4]

[1] Professor, McMaster University Centre for Effective Design of Structures, Department of Civil Engineering, Hamilton, Ontario, L8S 4L7 Canada, hamida@mcmaster.ca

[2] Research Associate, McMaster University Centre for Effective Design of Structures, Department of Civil Engineering, Hamilton, Ontario, L8S 4L7 Canada, eldak@mcmaster.ca

[3] Senior Engineer, Bechtel Power Corporation, Frederick, Maryland, 21703, USA, hakam@bechtel.com

[4] Professor, Civil, Architectural and Environmental Engineering Department, Drexel University, Philadelphia, PA, 19104, USA, elgaaly@drexel.edu

ABSTRACT

An experimental investigation was conducted to study the behaviour of unreinforced masonry (URM) walls retrofitted with composite laminates. Five masonry-infilled steel frames were tested with and without retrofit. The composite laminates increased the stiffness and strength and enhanced the post peak behaviour by stabilizing the masonry walls and preventing their out-of-plane spalling. Tests reported in this paper demonstrate the efficiency of FRP laminates in improving the capacity of URM containing the hazardous URM damage, preventing catastrophic failure and maintaining the wall integrity even after significant structural damage.

KEYWORDS: composite masonry, concrete masonry, fibre reinforced plastics, infilled frames, retrofitting, seismic hazard

INTRODUCTION

A common type of construction in urban centres for low-rise and mid-rise buildings is unreinforced masonry (URM) walls filling the space bounded by the structural framing members. In general, URM infill walls have demonstrated poor performance record even in moderate earthquakes. Their behaviour is usually brittle with little or no ductility and they, typically, suffer various types of damage ranging from invisible cracking to crushing and, eventually, disintegration and total collapse. This behaviour constitutes a major source of hazard during seismic events and creates a major seismic performance problem facing designers today.

A strong earthquake introduces severe in-plane and out-of-plane forces to masonry walls which may lead to catastrophic collapse. However, the majority of work conducted to date [1-7] has been concentrated on the out-of-plane behaviour of URM walls strengthened with externally applied FRPs. Infill panels (or large portions of wall) may fall out of the surrounding frame due to inadequate out-of-plane restraint at the frame-infill interface, or due to out-of-plane flexural or shear failure of the infill panel. In undamaged infills, these failures may result from out-of-plane inertial forces, especially for infills at higher story levels and with large slenderness ratios.

However, it is more likely for out-of-plane failure to occur after the masonry units become dislodged due to damage from in-plane loading [8].
The work presented herein investigates the effects of applying FRP laminates on the in-plane behaviour of URM masonry infill walls. The objective is to demonstrate the potential of the FRP on enhancing the shear and compressive strength of URM infill walls and preventing brittle collapse by means of stabilizing the face shell even after excessive damage. This would also maintain the wall's structural integrity and would reduce the possibility of URM walls collapsing and spalling, which is a major source of hazard during earthquakes, even if the whole structure remained safe and functioning.

EXPERIMENTAL PROGRAM

The experimental program consisted of testing five single-story/single-bay, one-third scale, moment-resisting, structural steel frames infilled with unretrofitted and retrofitted hollow concrete block masonry walls. The frames were tested under displacement controlled diagonal loading to evaluate the behaviour of the composite frame-wall system.
To identify the different frames tested, each specimen was assigned a name according to the following notation: the first character is used to identify the steel section of the bounding frame whether S3×5.7 (**W**eak frame) or W6×15 (**S**trong frame). The second character describes the type of infill, if any, "B" refers to no wall (**B**are frame), "U" or "R," indicating whether the wall was **U**nretrofitted or **R**etrofitted, respectively.
For the stronger S-frames, the clear height between the beams and the clear span between the columns were similar to those of the W-frames. Moreover, the beam-column connections were also designed as full-moment-resisting and fabricated using complete-joint-penetration groove welds to weld the beam flanges to the column flanges while 3.0 mm fillet welds were used to weld the beam webs to the column flanges. However, due to the expected high diagonal-compressive loading force, 10 mm thick stiffener plates were welded using 3.0 mm fillet welds between the column flanges in order to prevent premature web buckling at the loaded ends. To maintain symmetry, similar plates were also welded at the four corners of the S-frames. Table 1 lists the structural properties of the weak and strong frame sections [9] and outlines the five frames tested.

Table 1 - Structural properties and test matrix of the steel frames

Structural Property	Weak (W) Frame S3×5.7	Strong (S) Frame W6×15
Depth	76 mm	152 mm
Flange Width	59 mm	152 mm
Strong Axis (X-axis):		
Elastic Moment of Inertia	1,049,000 mm^4	12,112,000 mm^4
Elastic Section Modulus	27,500 mm^3	159,300 mm^3
Plastic Section Modulus	31,950 mm^3	176,980 mm^3
Infill Type	**Specimen**	
Bare	**WB**	**-**
Unretrofitted	**WU**	**SU**
Retrofitted	**WR**	**SR**

MATERIAL PROPERTIES

The one-third-scale true-model blocks [10] used in this investigation were replicas of the standard, full-scale 150 mm wide hollow concrete masonry units [11]. The average net-area-based compressive strength of the blocks was 27.87 MPa. The masonry assemblages were constructed using scaled down mortar joints with a nominal thickness of 3.2 mm. To simulate actual construction practice, the mortar mix was designed as Type S mortar [12] and all mortar joints were tooled to a concave profile. The selected FRP was a bi-directional $0^{\circ}/90^{\circ}$ Glass-FRP with 0.295 kg/m^2 of E-glass fibers applied on both wall faces. The properties of the GFRP composites were determined according to ASTM D-3039 specification [13] and were supplied by the manufacturer. However, an average strength of 260 MPa (84% of the specified strength in the GFRP data sheet) with 8.0% C.O.V. was determined by testing five specimens according to the ASTM D-3039 [13]. The steel used for the steel frame sections was of A 36 grade (yield strength 243 MPa) for the **W**eak, W-Series, frames, and A572-50 (yield strength 379 MPa) for the **S**trong, S-Series, of frames.

TEST SETUP AND INSTRUMENTATION

The general test setup and loading assembly are shown in Figure 1-a. The compressive top load was applied using an AMSLER hydraulic jack with a load capacity of 490 kN and a maximum stroke of 125 mm. A lateral bracing system consisting of four L $6\times6\times{}^{3}/_{8}$ angles were used to prevent out-of-plane deformations during the in-plane loading of the frames.

Figure 1-b illustrates the typical instrumentation installed on the infill wall and bounding frame. The figure also shows the locations of the critical sections along the steel frame where strain gauges were placed (one of the W6×15 infilled steel frame is shown in the figure for illustration). All LVDTs, strain gauges, and the load cell used to measure the applied compressive load were all connected to a PC data acquisition system.

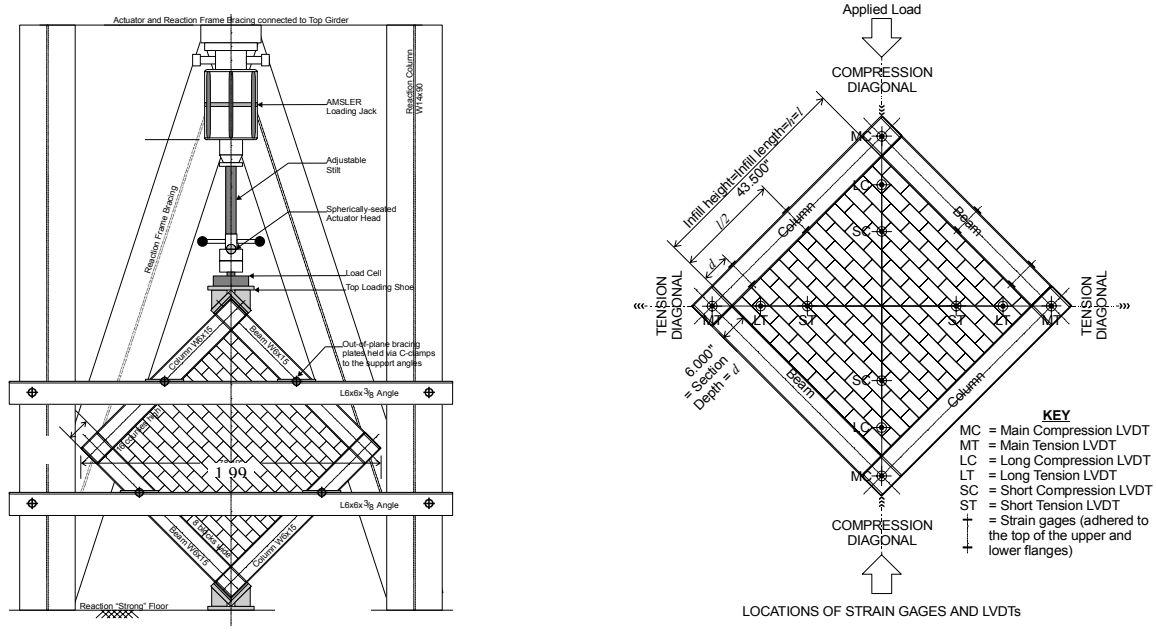

(a) **(b)**

Figure 1 - The masonry infilled steel frame specimens: a) test setup; b) instrumentation

TEST RESULTS

WB frame

As expected, the frame joints underwent severe rotation and distortion and behaved in an elastic-perfectly plastic manner. Both joints along the tension diagonal experienced tearing of the webs as shown in Fig. 2, and the frame suffered permanent (i.e., plastic) deformations. The initial stiffness obtained from the load-deflection curve (Figure 2) was 2.2 kN/mm. A linear behaviour was observed up to a load of a 25.8 kN corresponding to an average top displacement of 11.9 mm. Subsequently, a load plateau of 27.0 kN was attained at a top displacement of 14.0 mm. Attributed to the strain hardening effects, a slight increase in load occurred resulting in an ultimate load of 28.3 kN. The actual load-deflection behaviour closely resembles the expected behaviour in which an initial linear response occurs until initiation of yielding followed by a plateau then a slight load increase to attain the ultimate failure load.

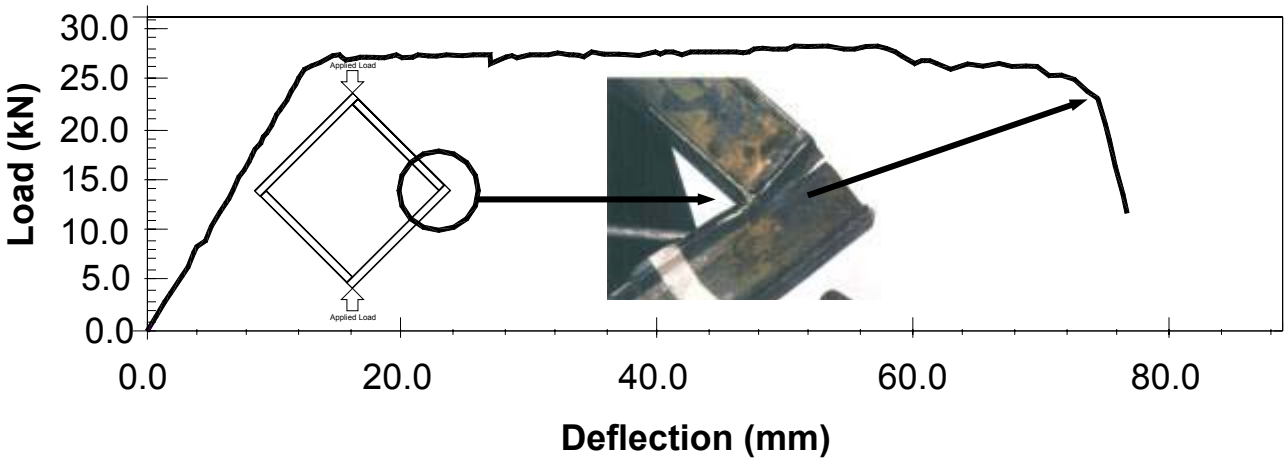

Figure 2 - Load-deflection relationship for frame WB

WU frame

The maximum load carrying capacity attained by the infilled frame was 104.0 kN. A stepped diagonal crack was observed at the center of the infill panel along the compression diagonal as shown in Figure 3-a. The crack was announced by an audible bang and occurred at a load of 7.8 kN corresponding to 7.5% of the maximum attained load. The load-deflection relation obtained for frame WU is shown in Fig. 3-a. The load versus deflection curve of the bare WB frame tested earlier is reproduced on the same plot for comparison.

Initially, the load-deflection curve was characterized by a steady rise up to a peak of 97.7 kN at corresponding deflection of 1.9 mm. Shortly afterwards, a major off-diagonal crack parallel to the initial toothed crack at the centre of the infill panel was observed at approximately 5.1 mm. Local cracking due to crushing of the infill in the vicinity of the bottom loading shoe occurred at approximately 7.6 mm. At approximately 15.0 mm, cracks along the infill bed joints were observed and propagated at mid-length of the frame columns until a significant portion of the infill panel face shell separated (approximately at 28.0 mm). Face shell spalling continued rapidly (at 33.0 mm) resulting in severe deterioration and cracking in the infill panel until the infill panel ceased to contribute in resisting the applied load (at 56.0 mm). The severity of the damage at the centre of the masonry infill is illustrated in Figure 3-b.

The infilled WU frame attained a maximum load carrying capacity of 104.0 kN which represents an increase of 267.5% compared to the capacity of the bare WB frame. The initial stiffness of the WU frame measured as the secant stiffness at 50% of the maximum load carrying capacity was determined as 55.7 kN/mm, which is 25 times that of the bare frame.

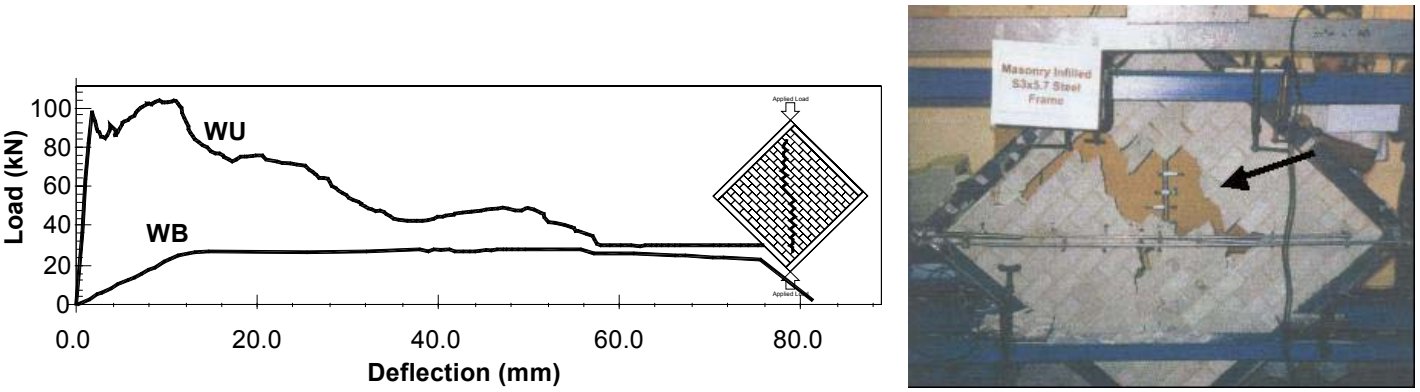

(a) **(b)**

Figure 3 - Frame WU: a) load-deflection relationship; b) damage at the infill centre

WR frame

The load versus deflection curves for the WR frame is shown in Figure 4-a. The maximum load attained by the frame was 218.9 kN which represents increases of 7.7 times and 2.2 times the maximum loads attained by the WB and WU frames respectively. At a load of 182.4 kN corresponding to 83.3% of the maximum load-carrying capacity, some hairline cracks were observed in the blocks near the vicinity of the top loading shoe. These cracks were visible underneath the clear laminate adhered on the exterior of the masonry infill panel. As the load began to decrease, cracking noises and clicks were heard until suddenly at a load of 175.1 kN, corresponding to 80.0% of the ultimate load on the descending branch of the load curve, the interior webs near the top portion of the infill panel were damaged causing the separated retrofitted face shells near the top loading shoe to snap outwards and moved outside the flanges of the frame members (Figure 4-b). Unfortunately, shortly before and after this outward "burst," the buckled face shell brushed against the main and infill compression LVDTs, thus preventing further recording of displacement.

A thorough understanding of the behaviour and response of the retrofitted infill panel was further facilitated upon its removal from the bounding steel frame thereby enabling a closer inspection. Figure 4-c shows the wall separation in the left side of the frame. The retrofit technique using FRP laminates was very successful in preserving the integrity of the highly brittle masonry. The fact that the panel, simulating a storey-high wall, was removed in one intact piece (in spite of some damage to the interior webs) is testimony to the beneficial effect of retrofit with FRP overlay. At the toes of the infill panel within the vicinity of the loaded corners of the frame, all interior webs were damaged. The secant stiffness at 50% of the maximum load, the initial stiffness of the BR frame is 131.4 kN/mm which represents increases of 58.7 times and 2.4 times the initial stiffness values of the WB and WU frames respectively. The peak load was reached at a compressive deflection of 5.6 mm. Similar to the WU frame, the recorded deflections along the

compression diagonal in the direction of the applied load were greater than those along the tension diagonal. This is attributed to the local cracking at the infill's loaded toes resulting in a reduced stiffness along the loading direction. Ultimately, as the infill panel was no longer in any effective contact with the bounding steel frame, a load plateau was attained which represents the bare frame's plastic load capacity. The load stabilized at a value of 28.9 kN which is comparable to the WB frame capacity.

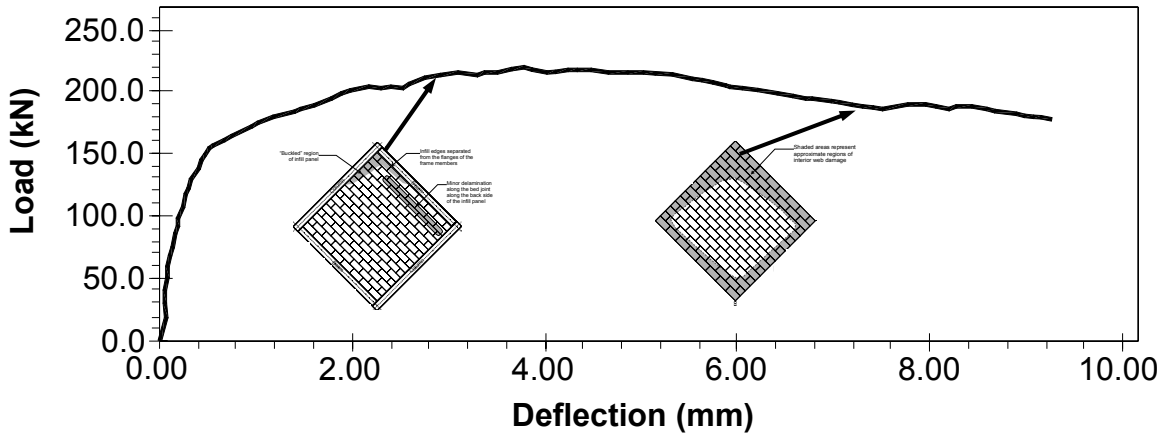

(a)

(b) **(c)**

Figure 4 - Frame WR: a) Load-deflection relationship; b) out-of-plane wall burst; and c) extent of web splitting

SU frame

A plot of the applied top load versus deflections for the SU frame is shown in Figure 5-a. The initial secant stiffness of the SU frame was 91.4 kN/mm. The ultimate load-carrying capacity of the SU frame determined in the second test was 284.4 kN. The unretrofitted masonry infill panel

remained crack-free up to an applied diagonal load of 122.4 kN corresponding to 43.0% of the ultimate load-carrying capacity of the SU frame. Thereafter, a longitudinal crack at the middle of the panel occurred similar to the WU frame. Near the peak load, signs of crushing of the boundary mortar joint between the steel frame and the infill panel in the vicinity of the loaded corners were observed. Moreover, a hairline separation crack between the panel and the frame at the tension corners was observed to extend approximately three courses long.

The cracking pattern of the masonry infill wall resembles that encountered in the WU frame test in which a central crack is first initiated along the loaded diagonal of the wall followed by the formation of some off-diagonal cracks. In the second test attempt, the existing but closed hairline cracks resulting from the first test widened as the frame reached a first peak load at 266.9 kN at a corresponding deflection of 6.8 mm. Shortly before reaching the peak load, minor cracking was observed in the infill's toe near the bottom loading shoe. As the frame was pushed further in spite of the decreased load resistance, small off-diagonal cracks began forming on the left and right sides of the central crack. These cracks assisted in the redistribution of the load within the infill panel as it adjusted to bear against the deforming shape of the steel frame. Suddenly, collapse of massive "chunks" of the upper region of the wall occurred, with only the lower three courses of the masonry wall remained standing on the lower beam and column of the frame as shown in Figure 5-b. As the load increased, the SU frame was simply behaving as a bare W6×15 moment-resisting frame and yielding commenced at the beam-column joints.

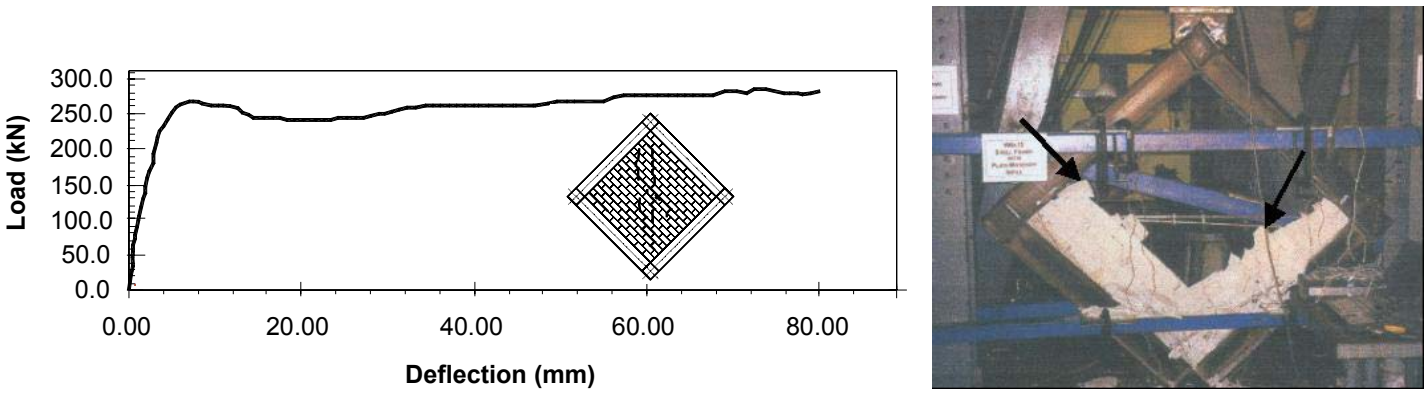

(a) **(b)**

Figure 5 - Frame SU: a) Load-deflection relationship and diagonal cracking; b) Collapse of the upper infill region

SR frame

Figure 6-a shows the load-deflection relationship of the SR frame. The SR frame's maximum load capacity was 343.0 kN and an initial stiffness of 262.7 kN/mm. At a deflection of 1.98 mm, the load increased until it reached the first peak of 270.1 kN. At this point, a loud bang was heard and crushing at the top loaded toe of the infill panel was observed. As in the retrofitted assemblages, crushing at the top toe of the retrofitted masonry infill panel involved damage of the interior webs leading to the laminated face shells snapping outwards. The damage extended along the infill-frame boundary for a length of approximately six courses (three block-lengths) and only one course wide (one half a block–length). A consequential loss in load capacity

occurred but gradually increased as the frame was further loaded. Similar crushing also occurred at the top loaded toe of the infill panel (Figure 6-b).
Separation between the infill panel and the steel frame at the tension diagonal corners occurred as loading progressed. The extent of toe crushing, which is defined as splitting of the face shell and at times accompanied by minor delamination between the overlay and the face shell itself, also increased (Figure 6-c). The steel frame was considerably deformed with significant plastic rotation at the tension joints. Examination of the infill panel at the end of the test (Figure 6-d) indicated that, other than minor delamination at the infill-frame boundaries and toe crushing and in spite of the separation between the infill and the frame at the tension diagonal corners, the central region of the wall was intact without any cracking or damage.

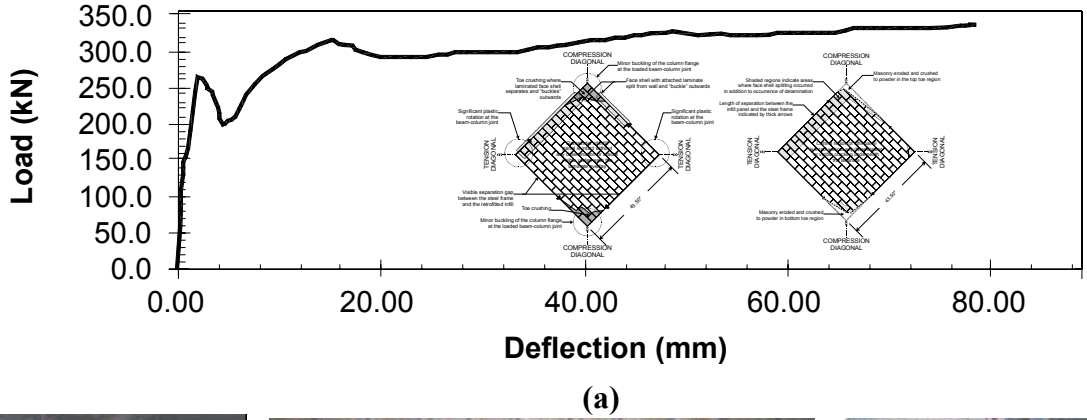

(a)

(b) **(c)** **(d)**

Figure 6 - Frame SR: a) Load-deflection relationship; b) Damage progress at top loaded corner; and c) Damage progress at bottom loaded corner d) Final damaged configuration

SUMMARY OF TEST RESULTS

Beside the local toe crushing, secondary signs of distress resulting from severe face shell splitting such as tearing of the laminate or minor delamination between the block face shells and the laminates were the only observed damages as the FRP retrofitted infilled-frames were pushed to severely deformed configuration. The frames with the retrofitted infill walls experienced similar behaviour throughout the entire loading history. In both the WR and SR tests, as soon as local crushing occurred at the wall's corners, clearly visible and wide separation gaps between the panel and the frame constantly increased unlike in the WU and SU frames. Unlike the

unretrofitted-masonry infill walls which disintegrated soon after the infilled-frame system reached its peak load, the retrofitted infill walls remained supported within the bounding steel frame until the end of the loading and even after attainment of load plateau which signalled that the frames reached the plastic load carrying capacity of the bare steel frame. This behaviour demonstrates the superior contribution of FRP laminates in altering the brittle hazardous behaviour of URM infill walls to a ductile and damage-tolerant wall with apparent post-peak capacity and energy dissipation capabilities.

Table 2 summarizes the maximum diagonal compressive load sustained by the five tested frames. In addition, the plastic load capacity of the bare W6×15 which was experimentally determined through testing the SU frame after the remains of the infill panel were removed (the third test of the SU frame) is also included in the table. The percentage and the corresponding multiple increases in the load-carrying capacity compared to that of the bare frame and the unretrofitted-masonry infilled frame for each of the two steel frame types are also calculated and presented in Table 2.

Table 2 also compares the initial secant stiffness of the five tested frames in this study. The stiffness values were calculated as the slope of line joining the origin and the point at 50% of the ultimate load using the applied diagonal load versus in-line compressive displacement curves. Although a bare W6×15 steel frame was not tested as a separate frame, its stiffness which is shown in Table 2 was experimentally determined from the second test of the SR frame whose infill panel was separated from the frame along the majority of its perimeter and sustained local damage at its loaded toes whereas the steel frame did not experience any distress in the prior test. For each frame within the two main steel frame types, the increases in stiffness compared to the bare frame and the first test of the unretrofitted-masonry infilled frame are computed and presented in the table.

Table 2 - Summary of the test results

Frame		Max Load (KN)	% Increase Compared to:		X's Increase Compared to:		Initial Secant Stiffness (kN/mm)	X's Increase Compared to	
			Bare Frame	Unretrofitted Infilled Frame	Bare Frame	Unretrofitted Infilled Frame		Bare Frame	Unretrofitted-Masonry Infilled Frame
W-Frames (S3×5.7)	WB	28.3					2.2		
	WU	104.0	267.5%		3.67		55.7	24.92	
	WR	219.0	673.9%	110.6%	7.74	2.11	131.4	58.74	2.36
S-Frames (W6×15)	SB	280.4(1)					20.9(1)		
	SU	284.4	1.4%		1.01		91.4	4.38	
	SR	343.1	22.4%	20.6%	1.22	1.21	175.1	8.40	1.92

(1) Plastic load carrying capacity and initial secant stiffness of the bare W6×15 frame was experimentally determined from the third test of the SU frame after the remains of the infill wall were removed entirely.

CONCLUSIONS

The following conclusions resulted from the investigation:

1. Retrofitting the infill panel with externally, epoxy-bonded FRP laminates resulted in an increase in load carrying capacity of 2.1 and 1.2 times that of the corresponding unretrofitted-masonry infilled frames for the W-frames and the S-frames respectively.
2. Even in the S-frames whose load capacity was not significantly increased due to retrofit of the infill panel, the laminates were able to completely alter the deformation characteristics and behaviour of the wall itself. In the unretrofitted-masonry infilled frames, the walls were completely destroyed and the blocks fell out-of-plane which in real life poses a hazard to buildings' occupants. The failure mode of the two unretrofitted frames was characterized as corner-crushing and diagonal-compression respectively. In the retrofitted masonry-infilled frames, no signs of diagonal cracking were observed and both frame types failed due to local crushing at the loaded corners. Examination of the retrofitted panel indicated that the central region remained intact and that the majority of the damage occurred at the outermost perimeter and at the loaded corners where the inner webs of the blocks cracked resulting in the formation of separate laminated-face shells.
3. The retrofitting technique maintained the walls structural integrity and prevented collapse and debris fallout. The FRP laminates contained and localized the damage of the URM walls even after ultimate failure and no signs of distress were evident throughout the wall except at the vicinity of the corners and around the openings. In contrast to the URM walls, the strengthened walls were stable after failure. In a real building, this can reduce the seismic hazard associated with the wall tipping off or falling out of the frame, and eliminate injuries or loss of lives and properties due to the wall collapse. This would also maintain the wall's structural integrity and would reduce the possibility of URM walls collapsing and spalling, which, in itself, is a major source of hazard during earthquakes, even if the whole structure remained safe and functioning.
4. The masonry-FRP composite walls do not fail catastrophically as their URM counterparts. The FRP laminates resulted in a gradual prolonged failure and a stronger wall with more energy dissipation and apparent post peak strength. This should result in a higher response modification factor than that typically selected for the analysis of URM structures.
5. By supplying the shear strength at the mortar joints, FRP laminates can serve as external reinforcement for unreinforced or under-reinforced masonry walls, thus providing a quick and cost-effective solution to conform to the more restrict emerging seismic codes requirements.

ACKNOWLEDGEMENTS

The work presented herein was supported under Grant No. CMS-9730646 from the National Science Foundation (NSF). The results, opinions, and conclusions expressed in this paper are solely those of the authors and do not necessarily reflect those of the NSF. The authors would like to gratefully acknowledge assistance of Edward Fyfe, Peter Milligan and Sarah Cruickshank, Fyfe Co. LLC, California, for providing the FRP, and John Sabia, D.M. Sabia Co., Pennsylvania for providing the mason.

REFERENCES

1. Triantafillou, T. C. (1998) "*Strengthening of Masonry Structures using Epoxy-Bonded FRP Laminates*," Journal of Composites for Construction, ASCE, Vol. 2, No. 2, May, pp. 96-104.
2. Velazquez-Dimas, J. I., and Ehsani, M. R (2000) "*Modeling Out-of-Plane Behavior of URM Walls Retrofitted with Fiber Composites*," Journal of Composites for Construction, ASCE, Vol. 4, No. 4, November, pp. 172-181.
3. Albert, M. L., Elwi, A. E. and Cheng, J. J. R. (2001) "*Strengthening of Unreinforced Masonry Walls Using FRPs*" Journal of Composites for Construction, ASCE Vol. 5, No. 2, pp. 76-84.
4. Hamoush, S. A. McGinley, M. W. Mlakar, P. Scott, D. and Murray, K. (2001) "*Out-of-Plane Strengthening of Masonry Walls with Reinforced Composites*" Journal of Composites for Construction, ASCE, Vol. 5, No. 3, pp. 139-145.
5. Hamilton III, H. R. and Dolan, C. W. (2001) "*Flexural Capacity of Glass FRP Strengthened Concrete Masonry Walls*" Journal of Composites for Construction, ASCE, Vol. 5, No. 3, August, pp. 170-178.
6. Kuzik, M.D., Elwi, A.E. and Cheng, J. J.R (2003) "*Cyclic Flexure Tests of Masonry Walls Reinforced with Glass Fiber Reinforced Polymer Sheets"* Journal of Composites for Construction, ASCE, Vol. 7, No. 1, February, pp. 20-30.
7. Tan, K.H. and Patoary, M. K. H. (2004) "*Strengthening of Masonry Walls against Out-of-Plane Loads Using Fiber-Reinforced Polymer Reinforcement*" Journal of Composites for Construction, ASCE, Vol. 8, No. 1, February, pp. 79-87.
8. FEMA-274, (1997), *NEHRP Commentary on the Guidelines for the Seismic Rehabilitation of Buildings*, Federal Emergency Management Agency, Washington, D.C.
9. AISC, (2003), American Institute of Steel Construction, 3rd ed., "*LRFD Manual of Steel Construction*", Chicago, Illinois.
10. Harris, H. G. and Sabnis, Gajanan M. (1999) "*Structural Modeling and Experimental Techniques*," second edition, CRC Press, New York.
11. American Society for Testing and Materials, ASTM C 90-92b, "*Standard Specification for Load-Bearing Concrete Masonry Units*," Annual Book of ASTM Standards, Vol. 04.05, West Conshohocken, Pennsylvania.
12. American Society for Testing and Materials, ASTM C 270-92a, "*Standard Specification for Mortar for Unit Masonry*," Annual Book of ASTM Standards, Vol. 04.05, West Conshohocken, Pennsylvania.
13. American Society for Testing and Materials, ASTM D 3039/D 3039M-93, "*Standard Test Method for Tensile Properties of Polymer Matrix Composite Materials*," Annual Book of ASTM Standards, Vol. 15.03, West Conshohocken, Pennsylvania.